Biodiesel Production from Macroalgae Oil from *Fucus vesiculosus* Using Magnetic Catalyst in Unconventional Reactor Assisted by Magnetic Field

Euripedes Garcia Silveira Junior [1] [iD]**, Lilian Fiori Boechat de Souza** [1]**, Victor Haber Perez** [1,*] [iD]**, Oselys Rodriguez Justo** [2]**, Euclésio Simionatto** [3] **and Lincoln Carlos Silva de Oliveira** [4]

[1] Center of Sciences and Agricultural Technologies (CCTA), State University of Northern of Rio de Janeiro (UENF), Campos dos Goytacazes 28013-602, RJ, Brazil
[2] Estácio de Sá University (UNESA), Campos dos Goytacazes 28020-740, RJ, Brazil
[3] Chemistry Department, State University of Mato Grosso do Sul (UEMS), Naviraí 79950-000, MS, Brazil
[4] Chemistry Institute, Federal University of Mato Grosso do Sul (UFMS), Campo Grande 79070-900, MS, Brazil
* Correspondence: victorh@uenf.br

Abstract: A novel magnetic catalyst with hollow cylinder shape based on $K_2CO_3/\gamma\text{-}Al_2O_3/Sepiolite/CoFe_2O_4$ was prepared to convert macroalgae oil (*Fucus vesiculosus*) into biodiesel in an unconventional reactor assisted by magnetic field. Catalysts were formulated by the extrusion and characterized satisfactorily by physicochemical (mechanical strength, XRD, TG/DTG, FTIR and $TPD\text{-}CO_2$), magnetic (VSM and EPR), morphological (SEM) and textural properties (BET). While their catalytic performance was also evaluated at 70 °C, oil: ethanol molar ratio 1:12 and 6 wt.% of catalyst using two different reaction systems for comparative purposes: (a) conventional stirred reactor and (b) fluidized bed reactor assisted by a magnetic field. The attained biodiesel presents properties in accordance with the standard limits (ASTM and EN) and total conversion (>99%) was observed in both cases after 2 h of reaction without significant differences between the two reactors. However, the magnetic properties of these catalysts allowed stabilization of the bed under a magnetic field and easy magnetic catalyst separation/recovery at the reaction end, showing their great potential for biodiesel production with regard to conventional process and thus, transforming it into a more sustainable technology.

Keywords: macroalgae oil; magnetic catalyst; biodiesel; unconventional reactor; magnetic field

1. Introduction

Currently, around 80% of the energy consumed in the world comes from petroleum and its derivatives [1]. Therefore, global warming caused by the constant use of these fuels is a concern, and has been constantly discussed by scientific communities and governments around the world. Global greenhouse gas emissions are already recorded at 52 $GtCO_2e$ (tons of carbon dioxide equivalent) and it is estimated that from 2030 onwards, emissions of these pollutants could reach 58 $GtCO_2e$ per year. However, it has been extensively discussed that to keep global warming below 1.5 °C, the emissions of these gases must be reduced up to 30 $GtCO_2e$ per year by 2030 [1]. Despite efforts to reach the desired levels on the world stage, the use of renewable energies and the inclusion of biofuels does not seem to exceed 20% of global consumption, even when the demand for biofuels, such as bioethanol, biodiesel, HVO, biogas and biobutanol, has increased each year. In the case of biodiesel production, which is the focus of this work, in 2020, its world production was 39 billion liters, and the largest producers were Indonesia, Brazil, the United States, Germany and France [2].

The main challenges for biodiesel production still involve the use of non-edible oils as raw material, new applications for the use of glycerol and technological improvements to

reduce the production cost, including the development of new industrial processes and heterogeneous catalysts with low cost, among others [3]. Soybeans have a large share in the production of biodiesel. In Brazil, for instance, it has been the major feedstock around two decades, essentially due to advances in genetic studies that have enabled the use of new varieties resistant to pests and soil and climatic conditions. There are, however, expectations that some non-edible oil plants will gain space in the biodiesel production chain in the coming years. Obviously, this will only take place as technological advances in agriculture are achieved, especially in regard to oil plants with higher energy density than soybeans, i.e., with higher oil content in the seeds, such as: forage turnip oil [4], rubber seed oil [5], macaw and Jatropha [6], jeriva [7] and rice bran oil [8], among others.

Moreover, the relevance of microalgae oil as feedstock for biodiesel production has also been extensively reported due to its high oil content [9–16]. However, further research is needed to reduce the processing costs for these biomasses. In fact, according to Draaisma et al. [17], one of the main economic hurdles associated with the conversion of microalgae to biofuels is the energy cost of harvesting them.

On the other hand, van Hal et al. [18] consider that the energy costs of harvesting are not so troublesome for macroalgae due to their larger size, although they do not present a significant content of lipids compared to microalgae. Besides, macroalgae, also known as seaweeds, are attractively evaluated as a feedstock nowadays for the production of biofuels, including biomethane [19–22]; bio-oil [23–25]; bioethanol [26–30] and biodiesel [31–39], and to attain several important bioproducts for chemical and pharmaceutical applications [40].

F. vesiculosus has already been explored for the production of bio-oil [24] and biomethane [21], thus, it may be interesting to explore its potential for biodiesel production with this macroalgae in mind as feedstock for an integrated process. In addition, this macroalgae oil may be an alternative to edible oils, seeking to mitigate the energy vs. food conflicts besides biorefinery applications. In recent years, our research group has been studying biofuel production by unconventional process, among which, reactors/bioreactors assisted by magnetic field stand out [41–45].

Thus, the aim of this work was to evaluate the potential of macroalgae oil from *F. vesiculosus* for biodiesel production by unconventional means, i.e., in a bioreactor assisted by magnetic field using a magnetic catalyst based on $K_2CO_3/\gamma\text{-}Al_2O_3/\text{Sepiolite}/CoFe_2O_4$ and ethanol by chemical transesterification.

2. Materials and Methods

2.1. Materials

Macroalgae (*Fucus vesiculosus*) oil was purchased from GRAN OILS (Santo André-SP, Brazil). Boehmite (Pural SB Sasol (Spain) containing 85% of Al_2O_3) was used as $\gamma\text{-}Al_2O_3$ precursor and sepiolite (Pansil 100-TOLSA, S.A.—SPAIN 60%) were used as permanent binder. Iron chloride II ($FeCl_2$) (Alfa Aesar—USA, 99.5%), cobalt chloride II ($CoCl_2$) (Sigma Aldrich Brazil, 97%), Iron chloride III ($FeCl_3$) (Sigma Aldrich, 99%) and sodium hydroxide (NaOH) (Sigma Aldrich Brazil) were used for magnetic particle synthesis. Potassium carbonate (K_2CO_3) (Scharlau—Spain, 99%) was used as active phase and anhydrous ethanol (C_2H_6O) (Scharlau—Spain, reagent grade) was used as reagent alcohol.

2.2. Experimental Methods

2.2.1. Cobalt Ferrites Synthesis

Cobalt ferrites nanoparticles were prepared by the co-precipitation method, as described by [45]. After synthesis, the cobalt ferrites nanoparticles were filtered and washed with deionized water to remove the chloride ions, then they were washed with ethanol to ensure the removal of all residues from the synthesis. Finally, the nanoparticles were dried at 80 °C under vacuum for 24 h to remove the ethanol, then calcined in muffle with air atmosphere.

2.2.2. Preparation of Magnetic Catalysts

Catalysts with magnetic properties were prepared by mixing 175 g of potassium carbonate, 400.2 g of Boehmite (precursor to γ-Al_2O_3), 97.5 g of sepiolite and 150 g of cobalt ferrites, then slowly adding water (423 g) until a homogeneous mass was attained, which was then extruded using an extruder (2209 model, from Bonnot Company, USA) at 9 rpm. The extruded catalysts were dried at 105 °C up to constant weight and subjected to calcination at 500 °C for 4 h, resulting in K_2CO_3/γ-Al_2O_3/Sepiolite/$CoFe_2O_4$.

2.2.3. Biodiesel Synthesis by Chemical Transesterification

The transesterification reaction was carried out using macroalgae oil with oil: ethanol molar ratio 1:12, but the catalyst mass was varied by 4, 6 and 8%, and the reaction temperature to 60, 70 and 80 °C, using two different reaction systems for comparison purposes: (1) conventional stirred tank glass reactor at 200 rpm; (2) reactor assisted by an extremely low frequency (ELF) magnetic field. The reactor is basically formed by a glass column with the jacket for temperature control of the reactional medium and height/diameter (H/D) ratio = 250/14 mm. The magnetic catalyst was subjected to the axial magnetic field at 12 mT with reactional medium recycle, as described by Silveira Junior et al. [44]. Biodiesel formation kinetics were monitored as a function of fatty acid ethyl esters (FAEEs) produced by gas chromatography using a Shimadzu GC 2014 instrument (Shimadzu, Japan). Briefly, the injector and detector temperatures were set at 250 °C. Nitrogenous was used as the carrier gas, with a flow of 3 mL/min. The chromatographic column used was a BD 6584 (15 m $\times$ 0.32 mm $\times$ 0.1 μm) that was kept at 50 °C for 1 min, heated to 180 °C at 15 °C/min, then to 300 °C at 7 °C/min, and maintained constant for 10 min. The quantitative analysis of the FAEEs was formed based on the "Relative Peak Areas Method" considering the area of the target component peak as a proportion of the total area from all detected peaks [46].

2.3. Analytical Methods

2.3.1. Magnetic Catalyst Characterization

Thermogravimetric Analysis (TG/DTG)

The Thermogravimetric and Derivative Thermogravimetric curves (TG/DTG) was obtained in a TGA-Q50 equipment (TA Instruments, New Castle, DE, USA). Approximately 10 mg of samples was added to platinum crucible of the 90 μL. The analysis was performed with heating rate of 10 °C min^{-1} from room temperature to 900 °C, under synthetic air atmosphere with a flow of 60 mL min^{-1} in the oven and 40 mL min^{-1} of nitrogen atmosphere in the balance. To ensure the accuracy of the results, before obtaining the TG/DTG curves, the equipment was calibrated for thermo mass balance adjustment with standard weights of 100 mg and 1000 mg and the temperature adjusted by determination of the Curie Point Temperature of Nickel (358 °C) [44,45].

Scanning Electron Microscopy (SEM)

Samples of not calcined and calcined catalysts were mounted on carbon adhesive tape affixed to aluminum stubs and subsequently coated with platinum in a Sputter Coater Device (BAL-TEC SCD 005 Cool Sputter Coater). The samples were viewed using a LEO EVO 40 XVP scanning electron microscope (Carl Zeiss, Germany) at 15 kV. Micrographs were obtained at a magnification of 1800$\times$ for a comparative structural analysis of cell units and tissue patterns.

X-ray Diffraction

Structural analysis was carried out by X-ray diffractometry (XRD, X'Pert PRO Theta/2theta, PANalytical, The Netherlands). The patterns were recorded over the angular range of 5–90° (2θ) with a step size of 0.0334° and a time per step of 100 s, using Cu Kα radiation (λ = 0.154056 nm) with a working voltage and current of 40 kV and 100 mA, respectively.

Magnetic Properties Analysis of the Magnetic Catalysts

The magnetic properties of the $CoFe_2O_4$ nanoparticles and magnetic catalyst were performed by magnetization measurements by vibrating-sample magnetometer (VSM) and EPR analysis. VSM analysis were carried out on a SQUID vibrating-sample magnetometer (Quantum Design® models MPMS 57, MPMS 7T) and the temperature and field dependence of the samples were recorded on a Quantum Design MPMS-XL superconducting quantum interference device (SQUID). ZFC/FC measurements were performed in the 0–330 K temperature ranges with an applied field of 10,000 Oe. While, the X-band EPR spectra were recorded in situ on a CW Bruker EMX 300 spectrometer equipped with a Bruker TE102 cavity and Advanced Research System Helitran temperature control unit (10–300 K). The microwave frequency was measured with a Hewlett–Packard 5246L electronic counter [44,45].

Mechanical Strength

The mechanical strength of the magnetic catalyst was measured using a dynamometer in terms of burst pressure (Chatillon, NY, USA, LTMC model) applied on the external surface of the magnetic catalyst up to their rupture, according to the Standard Test Method for Radial Crush Strength of Extruded Catalyst Particles (ASTM D6175-98).

B.E.T Analysis

Specific surface area was calculated from nitrogen adsorption/desorption isotherms obtained at −196 °C in an ASAP 2420 apparatus (Micromeritics Instrument Corp., GA, USA) [47,48].

Chemisorption Analysis (CO_2-TPD)

Chemisorption analysis was carried out through the temperature programmed desorption profiles of CO_2 (CO_2-TPD) using apparatus with a mass detector (AutoChem II 2920V4.01 model from Micromeritics Instrument Corp., GA-USA) as describe by Silveira Junior et al. [3].

2.3.2. Characterization of Macroalgae Oil and Biodiesel Quality

Color Analysis of Macroalgae Oil

The color of macroalgae oil was characterized by CIE-Lab space method using a Spectrophotometer (Hunterlab MiniScan XE Plus, Virginia, USA) calibrated to a standard white and black reflective plate to obtain L*, a*, and b* values. A D65 illuminant and a 10° standard observer were employed. The measurements were taken at two equidistant points in the equatorial region of the sun-exposed and non-exposed sides of the oil. The proportion of green oil color was determined in relation to the full change of the Hunter a parameter.

Macroalgae Oil Composition

The macroalgae oil composition was determined by gas chromatography using a Shimadzu GC 2014 instrument (Shimadzu, Japan). Briefly, the injector and detector temperatures were set at 250 °C. Nitrogenous was used as the carrier gas with a flow of 3 mL/min. The chromatographic column used was a BD 6584 (15 m × 0.32 mm × 0.1 μm) that was kept at 50 °C for 1 min, heated to 180 °C at 15 °C/min, then to 300 °C at 7 °C/min and maintained constant for 10 min. For quantitative analysis of the FAEEs formed, the C4–C24 standard FAEEs from Supelco was used.

Macroalgae Oil and Biodiesel Quality

Other physicochemical analyses were carried out to evaluate both the macroalgae oil properties and the biodiesel quality, according to several standard methods (US Standard-ASTM D6751 and European Standard-EN 14213). Thus, density (ASTM D1298), kinematic

viscosity (ASTM D445), acid number (ASTM D664) and oxidative stability (Rancimat test) at 110 °C (EN 14112) were considered.

3. Results

As previously described, this work had the novelty of producing biodiesel from macroalgae oil (*Fucus vesiculosus*) via ethanol by heterogeneous catalysis using extruded catalysts with magnetic properties. Regarding macroalgae, despite their oil yield being less than 10% by weight [31,34,36], the exploration of this type of raw material for biodiesel production is interesting due to its unsaturated fatty acid composition, which is around 85.73% (Figure 1a). This oil is relatively greenish in color (Figure 1b), as validated by colorimetric analysis according to CieLab color space (L* = 60 ± 0.05; a* = −20 ± 0.05 and b* = 70 ± 0.04). Furthermore, this oil has an acidity index of 2.66 mg KOH/g, which, being less than 3.0 mg KOH/g, does not need a previous step of esterification, and therefore, is an attractive raw material of good quality for biodiesel production. This result is even more important when compared to oils from other macroalgae sources reported in the literature, which have much higher acidity indexes, such as *Enteromorpha compressa* oil, which reaches 12.60 mg KOH/g [38]; oil of *Ulva fasciata*, which can present between 9.3–13.73 mg KOH/g [34,49] and oil of *Melanothamnus afaqhusainii*, which can reach up to 18.2 mg KOH/g [33].

(a)

(b)
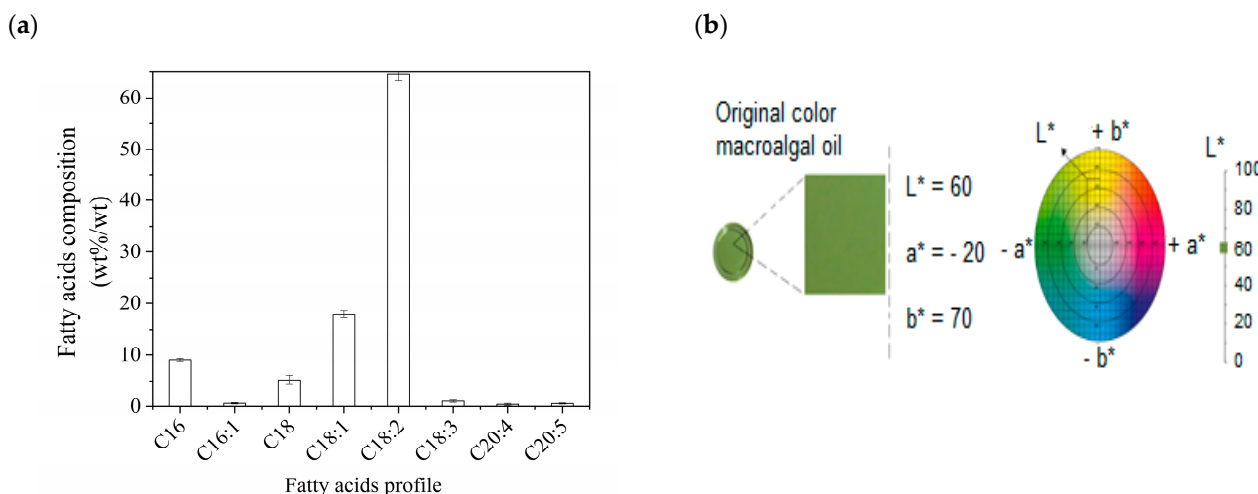
Figure 1. Macroalgae *Fucus vesiculosus* oil: (**a**) fatty acids profile determined by GC/FID analysis; (**b**) CieLab color analysis.

On the other hand, the catalyst developed for this study was an extruded derivative with the hollow cylindrical noodle geometry, whose basic dimensions are shown in Figure 2. This catalyst containing magnetic particles ($CoFe_2O_4$) was prepared to carry out chemical transesterification reactions from macroalgae oil and ethanol with oil: ethanol molar ratio 1:12 in a reactor assisted by magnetic field with axial field lines seeking by this way of magnetic catalysts stabilization inside the reactor.

Initially, the prepared catalyst was characterized from the structural point of view, and its thermal stability and morphology through XRD, FTIR, TG/DTG, and SEM analyses. Figure 3 shows the XRD diffractograms referring to the cobalt ferrite nanoparticles and the catalyst with magnetic properties. As can be seen, the cobalt ferrites have characteristic diffraction peaks corresponding to $CoFe_2O_4$, as corroborated by the Joint Committee on Powder Diffraction Standards (JCPDS #022-1086) and also in accordance with works reported in the literature [50,51]. In the case of the catalyst with magnetic properties, the active phase ($K_2Co_2Mg_3Si_{12}O_{30}$) in the catalyst was confirmed between 2θ = 20° and 40° (JCPDS #049-0361).
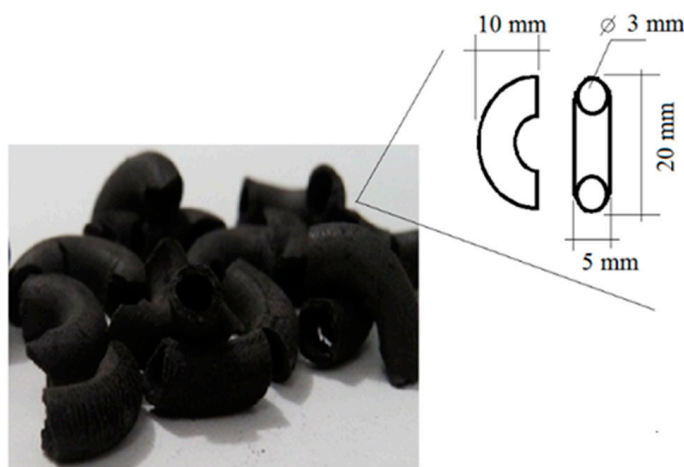
Figure 2. Geometric details of the catalysts K_2CO_3/γ-Al_2O_3/sepiolite/$CoFe_2O_4$ prepared by extrusion procedure.
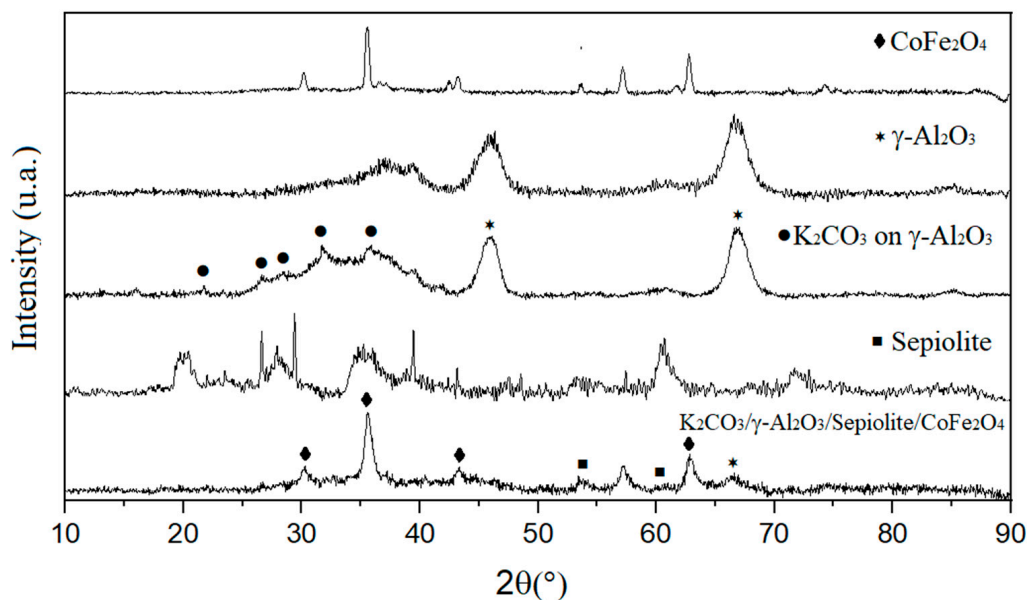
Figure 3. X-ray diffraction patterns of the cobalt ferrites and K_2CO_3/γ-Al_2O_3/sepiolite/$CoFe_2O_4$.

Figure 4 shows the thermal stability of the catalyst with magnetic properties according to the thermogravimetric analysis (TG/DTG). The thermal events that represent mass losses can be observed in the TG/DTG curves (the first up to 100 °C and the second around 200 °C), referring to free water and adsorbed water on the catalyst surface. While, around 450 °C, the loss of mass is attributed to structural water, that is, related to the decomposition of structural hydroxyl groups (-OH), and at this temperature range, there is a phase change from boehmite to γ-Al_2O_3 formation. At 800 °C, there is also a loss of mass due to the sepiolite thermodecomposition, resulting in enstatite. In addition, calcination temperatures below 800 °C do not affect the composition of the catalyst's active phase (K_2CO_3); however, above 850 °C, potassium carbonate releases CO_2, forming potassium oxide. Thus, 500 °C seems to be the proper calcination temperature for the final preparation of this catalyst, and obviously, the active phase in the form of K_2CO_3 on γ-Al_2O_3/Sepiolite/$CoFe_2O_4$ after calcination favors the formation of biodiesel at a reaction temperature of 70 °C [3].
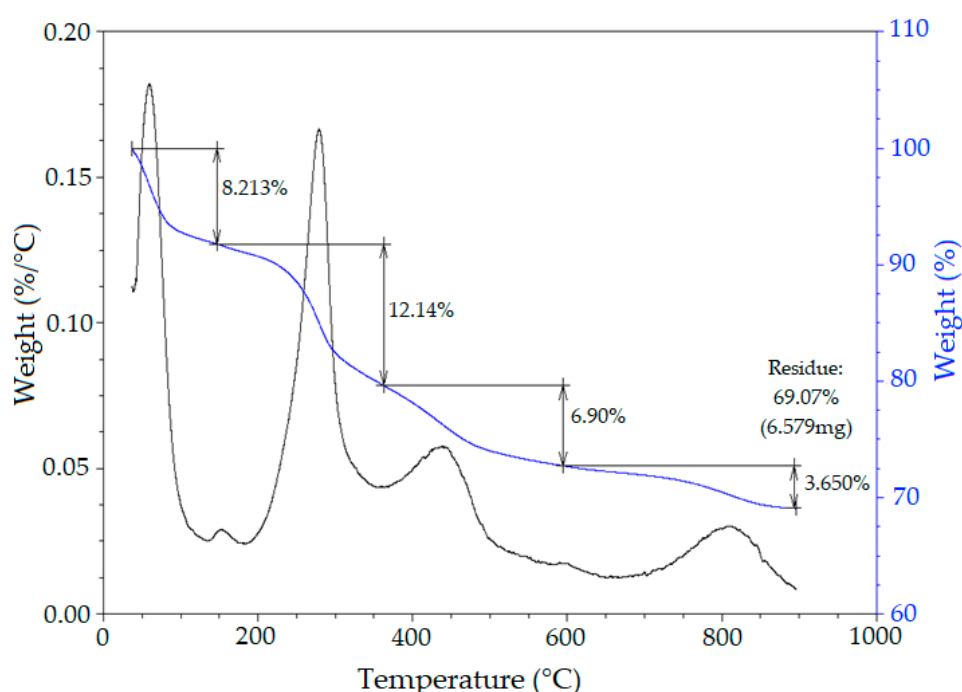
Figure 4. Thermogravimetric analysis (TGA-DTG) for $K_2CO_3/\gamma\text{-}Al_2O_3/\text{sepiolite}/CoFe_2O_4$.

Furthermore, by SEM analysis, it was also possible to confirm changes in the morphology of the catalyst after calcination (Figure 5). The sepiolite used in the catalyst composition acts as permanent binder between the active phase (K_2CO_3) and the support ($\gamma\text{-}Al_2O_3/CoFe_2O_4$). This additive has a fibrous structure that plays an important role in catalyst extrusion. After calcination, due to loss of water, it is possible to discriminate the clay fibers that vary between 10 to 20 μm in length, probably binding the components of the extruded catalyst. In addition, sepiolite not only acts as a binder, but also becomes a ceramic material after calcination, thus providing a high mechanical resistance to catalysts (Table 1).

(a)

(b)
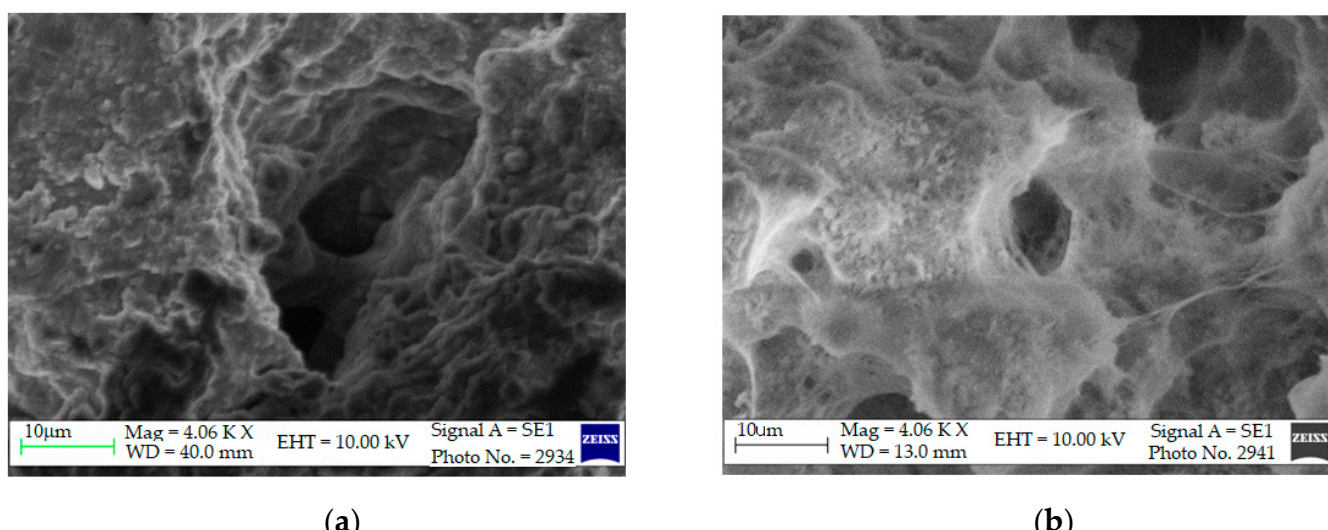
Figure 5. Micrographs attained by SEM with 1800× magnification for: (**a**) not calcined catalyst and (**b**) calcined catalyst.

Table 1. Physico-chemical properties of the prepared catalysts from K_2CO_3/γ-Al_2O_3/Sepiolite/$CoFe_2O_4$.

Physico-Chemical Properties	Values
Mechanical strength (kgf/cm)	3.12
Specific area (m^2/g) determined by BET analysis	30
Pore volume (cm^3/g) determined by BET analysis	0.11
Pore size (nm) determined by BET analysis	15.3
Basicity (mmol/g of CO_2) determined by CO_2-TPD	5.68
Density of basic sites (mmol/m^2)	0.15

After calcination, the catalyst was used in the synthesis of biodiesel, aiming to evaluate its performance during the oil transesterification reaction (Figure 6). Initially, a kinetic study was carried out at 70 °C with oil: ethanol molar ratio of 1:12 in a reactor under agitation at 200 rpm, but varying the catalyst mass by 4, 6 and 8 wt%. As can be seen in Figure 6a, 47.13% conversion was achieved at 2 h of reaction using just 4% by catalyst weight; however, when the catalyst mass was increased to 8%, the conversion was only 74%, while to 6 wt.%, the conversion was complete. This result can be associated with a moderate diffusional limitation caused when doubling the amount of catalyst in the reaction, i.e., from 4 to 8 wt.%. For this reason, 6 wt% of catalyst was adopted in the subsequent transesterification reactions. In fact, problems with the performance of heterogeneous catalysts in the production of biodiesel have already been reported in the literature due to the diffusional limitation caused by increased resistance to mass transfer in this complex reaction medium [52–54].


(**a**)

(**b**)
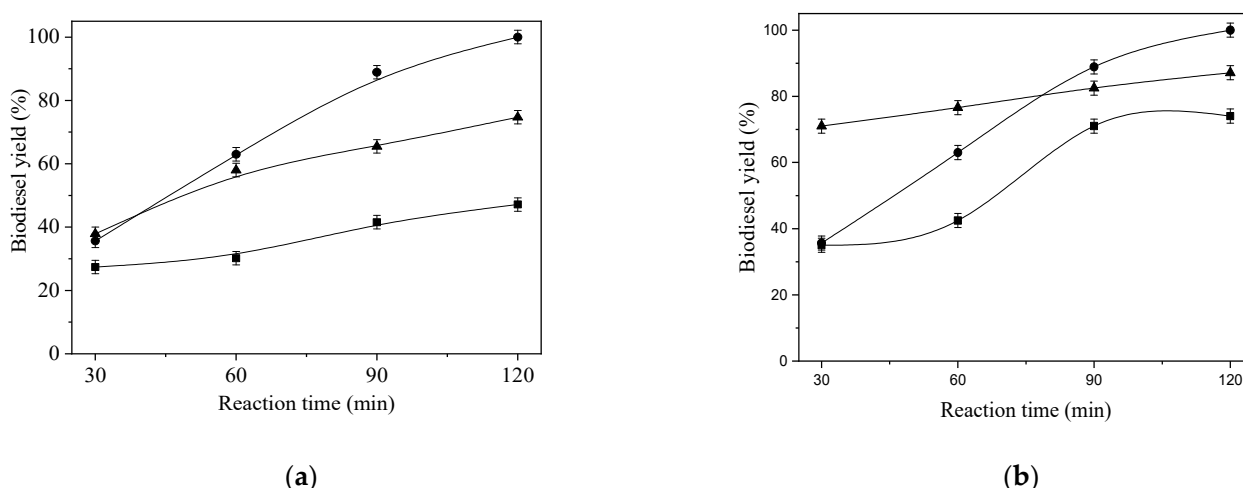
Figure 6. Biodiesel production from macroalgae *Fucus vesiculosus* oil, ethanol and K_2CO_3/γ-Al_2O_3/Sepiolite/$CoFe_2O_4$ catalyst. In (**a**) Reaction parameters: catalyst mass (■ 4%, ● 6% and ▲ 8%) at 70 °C, 200 rpm and 2 h reaction time; (**b**) Reaction parameters: reaction temperature (■ 60 °C, ● 70 °C and ▲ 80 °C), catalyst mass (6%), molar ratio (1:12) reaction time (2 h) and 200 rpm.

Thus, Figure 6b shows the formation of biodiesel by varying the reaction temperatures to 60, 70 and 80 °C in the reactor with agitation at the same molar ratio condition. In this case, the best result was observed when the reaction was carried out at 70 °C, reaching total conversion in 2 h of reaction. For a temperature of 80 °C, the reaction rate is initially faster, but the final conversion does not exceed 87%, probably due to the restrictions imposed on the system by the partial evaporation of ethanol at this temperature. This has already been observed by several authors [55–58] for reaction temperatures above the boiling point of ethanol, resulting in low conversion of oil into biodiesel.

The results described above can be considered satisfactory when comparing with other studies conducted with oils from different macroalgae varieties used in biodiesel synthesis (Table 2), in which the yields ranged from 70 to 97% using homogeneous and

heterogeneous catalysts for similar temperature and molar ratio conditions. Furthermore, the good performance of the catalyst developed in our study can be attributed to the basicity and basic sites density observed on the catalytic surface, whose values were 5.68 mmol/g and 0.15 mmol/m^2, respectively, obtained at the desorption temperature of 285 °C, which corresponds to basic sites of average strength (Table 1). In addition, the good performance of the catalyst can also be correlated with other physicochemical properties presented in Table 1. This catalyst with magnetic properties showed a satisfactory mechanical resistance since it preserved its structure after all reactions, thus facilitating separation and recovery step at the reaction end. Furthermore, in relation to textural properties, the low specific surface area obtained was a consequence of the extrusion process used in the catalyst's preparation; however, in this case, their basic sites content on the surface was more relevant for their good performance.

Table 2. Biodiesel production from macroalgae oil as feedstock by heterogeneous catalysis.

Macro Algae Oil	Catalysts	Reaction Parameters Oil: Alcohol Molar Ratio; Catalyst Weight (wt% or %); Temperature (°C); Stirring (rpm) or Flux (mL/min); Time (min)	Biodiesel Yield (%)	Ref.
Rhizoclonium sp.	NaOH	Oil: methanol (1:1); 1 wt% catalyst; 45 °C; 300 rpm; 180 min	82.2	[36]
Ulva linza	Mn$_2$ZnO$_4$	Oil: ethanol (1:12); 6 wt.% catalyst; 80 °C; magnetic stirrer; 240 min	72.3	[37]
Ulva tubulosa	Mn$_2$ZnO$_4$	Oil: ethanol (1:12); 6 wt.% catalyst; 80 °C; magnetic stirrer; 240 min	72	[37]
Ulva rigida	Mn$_2$ZnO$_4$	Oil: ethanol (1:12); 6 wt.% catalyst; 80 °C; magnetic stirrer; 240 min	70.4	[37]
Ulva reticulado	Mn$_2$ZnO$_4$	Oil: ethanol (1:12); 6 wt.% catalyst; 80 °C; magnetic stirrer; 240 min	71.5	[37]
Ulva lactuca	Clay-ZnO doped	Oil: methanol (1:9) 8% catalyst; 55 °C; continuous stirring; 50 min	97.43	[32]
Padina tetrastromatica	H$_2$SO$_4$ and CH$_3$ONa (two step reaction)	Oil: methanol (1:12); 1.5 wt% catalyst; 65 °C; 600 rpm; 120 min	96.2	[31]
Dictyota dichotoma	CaO, MgO, ZnO e TiO$_2$	Oil: methanol (1:18); 5 wt% catalyst; 65 °C; 600 rpm; 180	93.2	[35]
Melanothamnus afaqhusainii	CaO	Oil (5 g), methanol (10 mL) and catalyst (0.5 g); 100–110 °C; hot plate stirrer; 1080 min	80	[33]
Ulva fasciata	Waste industrial dusts containing CaO, MgO and ZnO	Oil: methanol (1:9) and catalyst (2 g); 80–100 °C; fast stirring; 360 min	88	[34]
Enteromorpha compressa	NaOH	Oil: methanol (1:9); 1% catalyst; 60 °C; 600 rpm; 90 min	90.6	[38]

Figure 7 comparatively shows the formation of biodiesel in two different reaction systems, i.e., conventional stirred reactor (Figure 7a), and unconventional reactor assisted by magnetic field (Figure 7b). As can be seen in the graphs, the results correspond to the formation of ethyl esters as a function of the fatty acid composition (FAEEs) of macroalgae oil (brought curves), as well as the overall yield of biodiesel for each system (continuous curve). In general, the profile of biodiesel formation under the conditions studied was similar between the different reaction systems, observing in all cases that there was complete conversion after 2 h of reaction without significant differences between the different reactors. However, during the reaction in the system with agitation, partial agglomeration of the catalytic particles was observed, which is an undesirable condition for the reuse of catalysts.

(a)
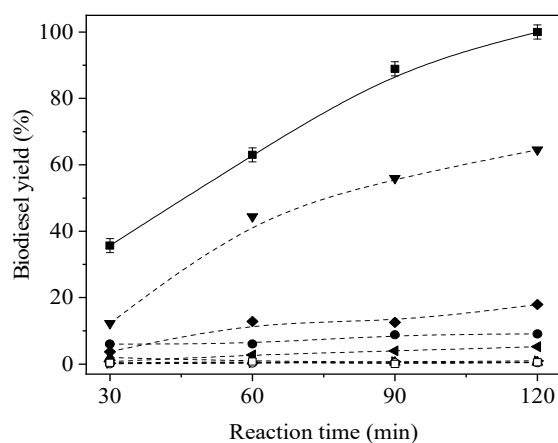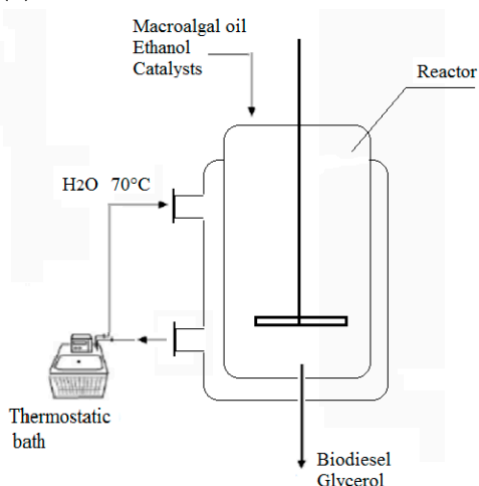
(b)
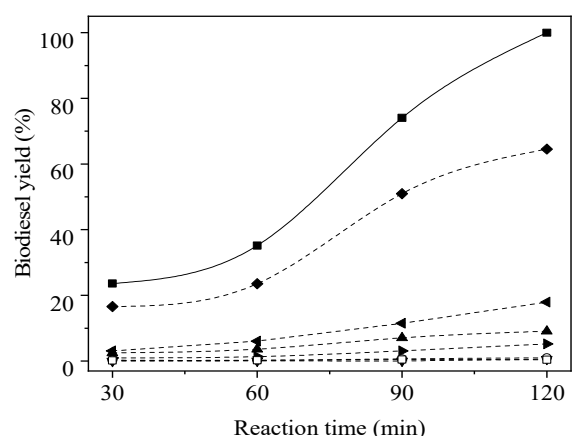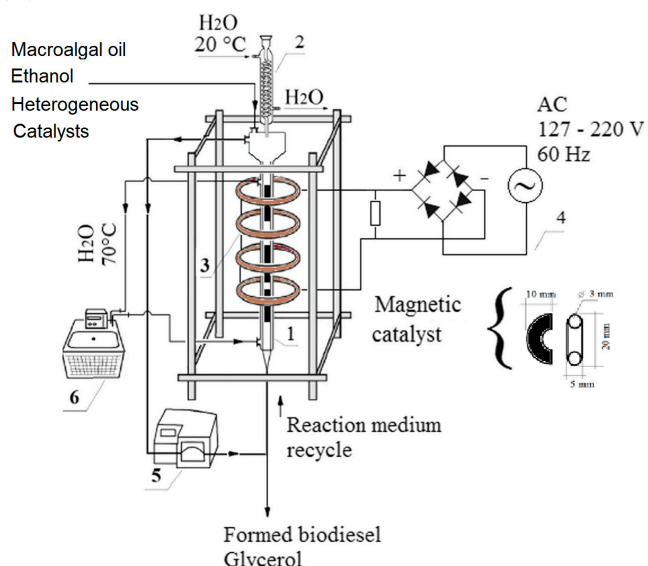
Figure 7. Biodiesel production from macroalgae *Fucus vesiculosus* oil, ethanol and K_2CO_3/γ-Al_2O_3/Sepiolite/$CoFe_2O_4$ catalyst with reaction parameters: catalyst mass (6%), molar ratio (1:12), reaction temperature (70 °C) and reaction time (2 h). In: (**a**) stirred reactor (200 rpm); (**b**) magnetically stabilized fluidized bed reactor with a recycle flow 7.69 mL/s and 12 mT (1- glass reactor; 2-condenser; 3-coils; 4 system for static magnetic field generation; 5- peristaltic pump for reactional medium recirculation and 6- thermostatic bath for reactor temperarure control). Symbols: ■ total biodiesel yield and fatty acid ethyl ester profiles (● C16; ▲ C16:1; ▼ C18:2; ◆ C18:1; ◄ C18; ► C18:3; ○ C20:4; □ C20:5).

While, in the absence of diffusional limitations, the reactor assisted by a magnetic field seems to be a good alternative among all systems, as it has the advantage of interacting with the magnetic properties of the catalysts and exploring strategies for homogeneous dispersion of the catalytic particles due to their magnetic stabilization in the reactional bed, as well as facilitating the separation/recovery of the catalyst at the end of the reaction step and, when desired, their reuse in several reactional cycles, depending on its magnetic properties and operating conditions that include the parameters of magnetic field intensity, as long as, its catalytic properties are preserved.

An important aspect that must be taken into account in these systems is the direction of the field lines, because when they are oriented in the axial direction, but in countercurrent

flow respect to the reactional medium, as the magnetic field strength increases, the catalyst gradually aligns itself magnetically in the direction of the field lines, thus contributing negatively to a gradual compaction in the catalytic bed. This fact has already been reported by Chen et al. [59], who evaluated the effect of magnetic field strength from 60 to 220 Oe on biodiesel production from waste cooking oil in a fluidized bed reactor assisted by a magnetic field.

Figure 8 shows the magnetic characterization for both particles of $CoFe_2O_4$ and catalysts (K_2CO_3/γ-Al_2O_3/Sepiolite/$CoFe_2O_4$) by VSM analysis. Cobalt ferrites exhibit superparamagnetic behavior, as indeed observed in Figure 8a. The magnetization versus field strength curves (M vs. H) show saturation at high fields and lack any hysterical behavior at low fields, with the absence of any detectable remanent magnetization [44]. It should also be noted in Figure 8b that magnetization decreases 6-fold with respect to the value observed for cobalt ferrites (from 49.82 to 8.30 emu/g). This low catalyst magnetization is probably related to the mass of cobalt ferrite that was effectively incorporated into the catalyst composition during extrusion, i.e., 0.3 g of $CoFe_2O_4$ for each gram of K_2CO_3/γ-Al_2O_3/Sepiolite.


(**a**)

(**b**)
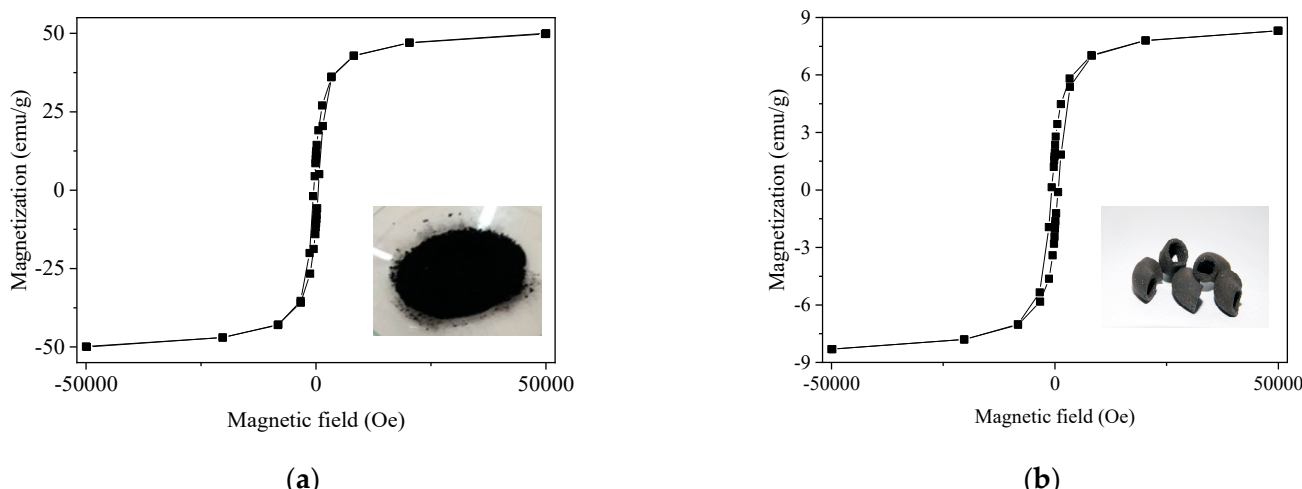
Figure 8. Magnetic characterization by VSM analysis for: (**a**) cobalt ferrites ($CoFe_2O_4$) particles and (**b**) K_2CO_3/γ-Al_2O_3/sepiolite/$CoFe_2O_4$. Analysis conditions: M vs. T, give H 748 = 10,000 Oe as applied field and for the M vs. H, give T = 300 K.

Regarding the magnetic properties evaluated by EPR analysis for $CoFe_2O_4$ and catalysts (K_2CO_3/γ-Al_2O_3/Sepiolite), both systems showed broad anisotropic signals at low temperatures, which are characteristic of ferromagnetic particles of different sizes and/or shapes (Figure 9). These results complement the VSM analysis, making it possible to verify that the profile of the EPR spectra obtained suggests that the prepared $CoFe_2O_4$ nanoparticles presented different sizes and shapes, resulting in highly agglomerated nanoparticles that present strong dipolar interactions and whose high value of g = 3.76 can be mainly attributed to the exchange between Fe^{3+} and Co^{2+} [60]. Similarly, the same phenomenon happens for the magnetic catalyst; however, it shows a slightly lower g value, probably due to the lower concentration of irregularly dispersed magnetic particles in the catalyst. Thus, according to the results obtained by VSM and EPR, it can be considered that the superparamagnetic properties of the catalysts prepared were satisfactory to their magnetic stabilization during the transesterification reaction and separation and catalyst recovery when the biodiesel production was completed.
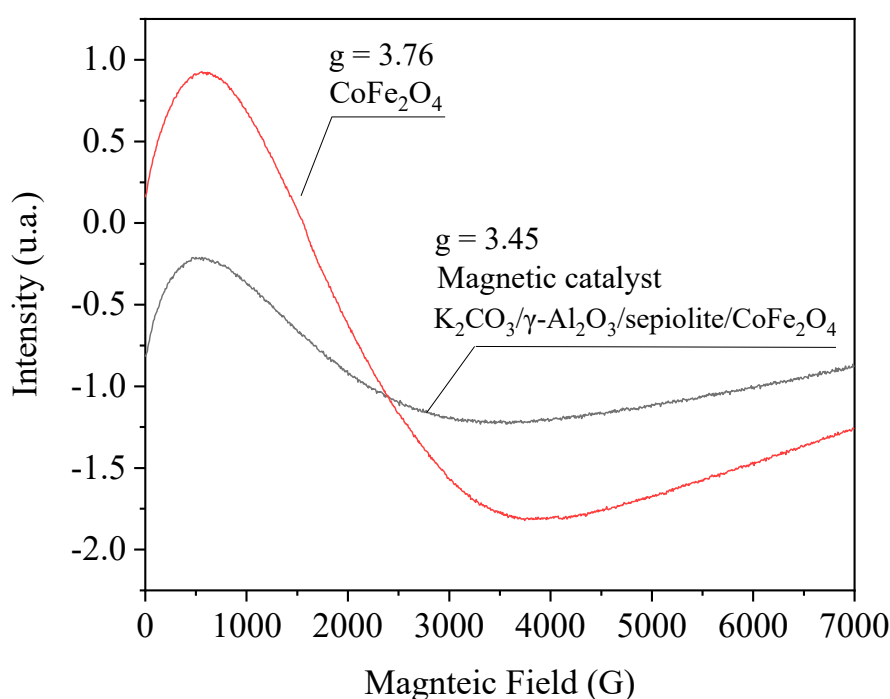
Figure 9. EPR spectra recorded at 298 K for $CoFe_2O_4$ and K_2CO_3/γ Al_2O_3/sepiolite/$CoFe_2O_4$.

The use of magnetic catalysts in biodiesel production has been studied extensively over the last decade, but in most cases, with applications in conventional reaction systems, and referring only to the use of magnets as a method of separating catalysts from the reaction medium [61]. Thus, few studies have reported the use of reactors assisted by magnetic fields in the production of biodiesel (Table 3) in which their application goes beyond the simple action of separation/recovery of the catalysts from the reaction medium by the field strength, i.e., considering that the interaction between the magnetic catalyst with the magnetic fields generated inside the reactor can contribute favorably to the magnetic stabilization of the reaction bed, and thus, avoid the diffusional limitations of heat and mass transfer often observed in conventional reactors [41].

In addition, the use of coupled systems with magnetic field generators has also been satisfactorily applied to different species of microalgae, such as *Chlorella homosphaera*, *Nannochloropsis oculata*, *Chlorella pyrenoidosa*, *Cunninghamella echinulate* and *Chlorella kessleri* to investigate the influence of the magnetic field on the production of biomass and lipids [62–66], which demonstrate great potential for biodiesel production.

Finally, the quality of biodiesel produced from *Fucus vesiculosus* was confirmed by several properties (Table 4) whose values were in accordance with the standard specifications (ASTM and EN). However, due to the low induction period of biodiesel, determined by Rancimat test, it is observed that the produced biodiesels showed low oxidative stability (1 h), which can be a consequence of their high content of unsaturated fatty acid esters. Despite this low oxidative stability of the *Fucus vesiculosus* oil esters, this does not preclude the use of these esters as inputs for biofuels. Alternatives, such as the use of additives and preparation of blends with oils that have good thermal and oxidative stability, can contribute to the use of this oil [67–69]. Recent research shows that optimizing fatty acid profiles by blending biodiesel from different sources and compositions can result in high quality fuels [70,71].

Table 3. Biodiesel production from several feedstocks in reactors assisted by magnetic field.

Feedstock	Catalyst	Reactor Type	Fluid Flow Rate and a Magnetic Field Intensity	Biodiesel Yield (%)	Ref.
Macroalgae *Fucus vesiculosus* oil	K_2CO_3/γ-Al_2O_3/Sepiolite/$CoFe_2O_4$ (hollow cylindrical noodle geometry)	Reactor assisted by magnetic field	750 mL/min and 12 mT	99.8	This study
Soybean oil	K_2CO_3/γ-Al_2O_3/Sepiolite/γ-Fe_2O_3 (magnetic monolithic catalyst)	Reactor assisted by magnetic field	16.6 mL/min and 2.5 mT	98.07	[44]
Sunflower oil	K_2CO_3/γ-Al_2O_3/Sepiolite/Fe_3O_4 (pellets)	*Reactor assisted by magnetic field	*The reactor assisted by magnetic field was used for magnetic catalyst separation.	88	[45]
Coconut oil	*Pseudomonas fluorescens* immobilized on chitosan with magnetic particles (microspheres)	Bioreactor assisted by electromagnetic field (differential mode reactor)	10.3 mL/min and 9.7 mT	12	[41]
Waste cooking oil	*Pseudomonas mendocina immobilized* in magnetic microspheres	magnetically fluidized bed reactor	16.97 mL/min and 136.63 Oe (13.67 mT)	91.8	[59]
Soybean oil	*Rhizopus oryzae* immobilized on chitosan with magnetic particles (microspheres)	Magnetically stabilized fluidized bed reactor (MSFBR)	25 mL/min and 150 Oe (15 mT)	91.3	[72]

Table 4. Physicochemical properties of macroalgal *Fucus vesiculosus* oil and biodiesel.

Properties	Standard Methods	Macroalgal Oil	Biodiesel
Density (kg/m^3) at 20 °C	ASTM D1298	922	870
Kinematic viscosity (mm^2/s) at 40 °C	ASTM D445	42.3	4.3
Oxidative stability, 110 °C	EN 14112	–	1 h
Acid number (mg NaOH/g)	ASTM D664	2.66	0.5

4. Conclusions

The development and improvement of unconventional methods for biodiesel preparation have been constantly studied. In this context, ethanolic biodiesel synthesis was satisfactorily carried out by chemical transesterification of Fucus vesiculosus oil and magnetic catalyst based on K_2CO_3/γ-Al_2O_3/Sepiolite/$CoFe_2O_4$ obtaining a total conversion at 2 h reaction. The quality of the produced biodiesel was validated according to ASTM and EN specifications and it was observed that all analyzed properties were in accordance with the standard limits. Although further studies are needed to evaluate the techno-economic viability of this unconventional process, this paper shows the potential of Fucus vesiculosus as feedstock for biodiesel production, despite its lipid content. Finally, according to the attained results, the developed magnetic catalyst can be considered as an attractive alternative for biodiesel production at industrial scale.

References

1. IPCC. *Global Warming of 1.5 °C*; An IPCC Special Report on the Impacts of Global Warming of 1.5 °C above Pre-Industrial Levels and Related Global Greenhouse Gas Emission Pathways, in the Context of Strengthening the Global Response to the Threat of Climate Change, Sustainable Development, and Efforts to Eradicate Poverty; Masson-Delmotte, V., Zhai, P., Pörtner, H.-O., Roberts, D., Skea, J., Shukla, P.R., Pirani, A., Moufouma-Okia, W., Péan, C., Pidcock, R., et al., Eds.; Cambridge University Press: Cambridge, UK; New York, NY, USA, 2018; p. 616. [CrossRef]
2. REN21. *Renewables 2021 Global Status Report (Paris: REN21 Secretariat)*; REN21: Paris, France, 2021; ISBN 978-3-948393-03-8.
3. Silveira Junior, E.G.; Perez, V.H.; Reyero, I.; Serrano-Lotina, A.; Justo, O.R. Biodiesel production from heterogeneous catalysts based K₂CO₃ supported on extruded γ-Al₂O₃. *Fuel* **2019**, *241*, 311–318. [CrossRef]
4. Silveira, E.G.; Barcelos, L.F.T.; Perez, V.H.; Justo, O.R.; Ramirez, L.C.; Filho, L.d.M.R.; de Castro, M.P.P. Biodiesel production from non-edible forage turnip oil by extruded catalyst. *Ind. Crops Prod.* **2019**, *139*, 111503. [CrossRef]
5. Roschat, W.; Siritanon, T.; Yoosuk, B.; Sudyoadsuk, T.; Promarak, V. Rubber seed oil as potential non-edible feedstock for biodiesel production using heterogeneous catalyst in Thailand. *Renew. Energy* **2017**, *101*, 937–944. [CrossRef]
6. Carvalho, A.K.F.; da Rós, P.C.M.; Teixeira, L.F.; Andrade, G.S.S.; Zanin, G.M.; de Castro, H.F. Assessing the potential of non-edible oils and residual fat to be used as a feedstock source in the enzymatic ethanolysis reaction. *Ind. Crops Prod.* **2013**, *50*, 485–493. [CrossRef]
7. Moreira, M.A.C.; Arrúa, M.E.; Antunes, A.; Fiuza, T.; Costa, B.J.; Neto, P.W.; Antunes, S.R.M. Characterization of *Syagrus romanzoffiana* oil aiming at biodiesel production. *Ind. Crops Prod.* **2013**, *48*, 57–60. [CrossRef]
8. Zullaikah, S.; Lai, C.-C.; Vali, S.R.; Ju, Y.-H. A two-step acid-catalyzed process for the production of biodiesel from rice bran oil. *Bioresour. Technol.* **2005**, *96*, 1889–1896. [CrossRef]
9. Ahmad, S.; Chaudhary, S.; Pathak, V.V.; Kothari, R.; Tyagi, V.V. Optimization of direct transesterification of *Chlorella pyrenoidosa* catalyzed by waste egg shell based heterogenous nano—CaO catalyst. *Renew. Energy* **2020**, *160*, 86–97. [CrossRef]
10. Das, V.; Tripathi, A.M.; Borah, M.J.; Dunford, N.T.; Deka, D. Cobalt-doped CaO catalyst synthesized and applied for algal biodiesel production. *Renew. Energy* **2020**, *161*, 1110–1119. [CrossRef]
11. Li, Y.; Lian, S.; Tong, D.; Song, R.; Yang, W.; Fan, Y.; Qing, R.; Hu, C. One-step production of biodiesel from Nannochloropsis sp. on solid base Mg–Zr catalyst. *Appl. Energy* **2011**, *88*, 3313–3317. [CrossRef]
12. Teo, S.H.; Islam, A.; Taufiq-Yap, Y.H. Algae derived biodiesel using nanocatalytic transesterification process. *Chem. Eng. Res. Des.* **2016**, *111*, 362–370. [CrossRef]
13. Turkkul, B.; Deliismail, O.; Seker, E. Ethyl esters biodiesel production from Spirulina sp. and Nannochloropsis oculata microalgal lipids over alumina-calcium oxide catalyst. *Renew. Energy* **2020**, *145*, 1014–1019. [CrossRef]
14. Umdu, E.S.; Tuncer, M.; Seker, E. Transesterification of *Nannochloropsis oculata* microalga's lipid to biodiesel on Al₂O₃ supported CaO and MgO catalysts. *Bioresour. Technol.* **2009**, *100*, 2828–2831. [CrossRef] [PubMed]
15. Lee, J.W.Y.; Chia, W.Y.; Ong, W.-J.; Cheah, W.Y.; Lim, S.S.; Chew, K.W. Advances in catalytic transesterification routes for biodiesel production using microalgae. *Sustain. Energy Technol. Assess.* **2022**, *52*, 102336. [CrossRef]
16. Manzoor, M.; Hussain, A.; Ahmad, Q.-u.-A.; Chaudhary, A.; Schenk, P.M.; Deepanraj, B.; Show, P.L. Biodiesel quality assessment of microalgae cultivated mixotrophically on sugarcane bagasse. *Sustain. Energy Technol. Assess.* **2022**, *53*, 102359. [CrossRef]
17. Draaisma, R.B.; Wijffels, R.H.; Slegers, P.; Brentner, L.B.; Roy, A.; Barbosa, M.J. Food commodities from microalgae. *Curr. Opin. Biotechnol.* **2013**, *24*, 169–177. [CrossRef] [PubMed]

18. van Hal, J.; Huijgen, W.; López-Contreras, A.M. Opportunities and challenges for seaweed in the biobased economy. *Trends Biotechnol.* **2014**, *32*, 231–233. [CrossRef]

19. Gruduls, A.; Maurers, R.; Romagnoli, F. Baltic Sea seaweed biomass pretreatment: Effect of combined CO$_2$ and thermal treatment on biomethane potential. *Energy Procedia* **2018**, *147*, 607–613. [CrossRef]

20. Ometto, F.; Steinhovden, K.; Kuci, H.; Lunnbäck, J.; Berg, A.; Karlsson, A.; Handå, A.; Hallan, H.; Ejlertsson, J. Seasonal variation of elements composition and biomethane in brown macroalgae. *Biomass Bioenergy* **2018**, *109*, 31–38.

21. Romagnoli, F.; Pastare, L.; Sabūnas, A.; Bāliņa, K.; Blumberga, D. Effects of pre-treatment on Biochemical Methane Potential (BMP) testing using Baltic Sea *Fucus vesiculosus* feedstock. *Biomass Bioenergy* **2017**, *105*, 23–31. [CrossRef]

22. Sheng, Y.; Shanmugam, S.; Chinnathambi, A.; Salmen, S.H.; Ge, S.; Xia, C.; Brindhadevi, K. Feasibility of microalgal and macroalgal biomass co-digestion on biomethane production. *Int. J. Hydrog. Energy* **2022**, *47*, 37394–37400. [CrossRef]

23. Jaiswal, K.K.; Kumar, V.; Vlaskin, M.S.; Nanda, M.; Verma, M.; Ahmad, W.; Kim, H. Hydropyrolysis of freshwater macroalgal bloom for bio-oil and biochar production: Kinetics and isotherm for removal of multiple heavy metals. *Environ. Technol. Innov.* **2021**, *22*, 101440. [CrossRef]

24. Jazie, A.A.; Haydary, J.; Abed, S.A.; Al-Dawody, M.F. Hydrothermal liquefaction of *Fucus vesiculosus* algae catalyzed by Hβ zeolite catalyst for Biocrude oil production. *Algal Res.* **2022**, *61*, 102596. [CrossRef]

25. Vimali, E.; Gunaseelan, S.; Devi, V.C.; Mothil, S.; Arumugam, M.; Ashokkumar, B.; Moorthy, I.M.G.; Pugazhendhi, A.; Varalakshmi, P. Comparative study of different catalysts mediated FAME conversion from macroalga *Padina tetrastromatica* biomass and hydrothermal liquefaction facilitated bio-oil production. *Chemosphere* **2022**, *292*, 133485. [CrossRef] [PubMed]

26. Cappelli, A.; Gigli, E.; Romagnoli, F.; Simoni, S.; Blumberga, D.; Palerno, M.; Guerriero, E. Co-digestion of Macroalgae for Biogas Production: An LCA-based Environmental Evaluation. *Energy Procedia* **2015**, *72*, 3–10. [CrossRef]

27. Dave, N.; Selvaraj, R.; Varadavenkatesan, T.; Vinayagam, R. A critical review on production of bioethanol from macroalgal biomass. *Algal Res.* **2019**, *42*, 101606. [CrossRef]

28. Dave, N.; Varadavenkatesan, T.; Selvaraj, R.; Vinayagam, R. Modelling of fermentative bioethanol production from indigenous *Ulva prolifera* biomass by Saccharomyces cerevisiae NFCCI1248 using an integrated ANN-GA approach. *Sci. Total Environ.* **2021**, *791*, 148429. [CrossRef] [PubMed]

29. Morimoto, K.; Chiou, T.-Y.; Konishi, M. Torulaspora quercuum shows great potential for bioethanol production from macroalgal hydrolysate. *Bioresour. Technol. Rep.* **2022**, *17*, 100952. [CrossRef]

30. Ruangrit, K.; Chaipoot, S.; Phongphisutthinant, R.; Kamopas, W.; Jeerapan, I.; Pekkoh, J.; Srinuanpan, S. Environmental-friendly pretreatment and process optimization of macroalgal biomass for effective ethanol production as an alternative fuel using *Saccharomyces cerevisiae*. *Biocatal. Agric. Biotechnol.* **2021**, *31*, 101919. [CrossRef]

31. Ashokkumar, V.; Salim, M.R.; Salam, Z.; Sivakumar, P.; Chong, C.T.; Elumalai, S.; Suresh, V.; Ani, F.N. Production of liquid biofuels (biodiesel and bioethanol) from brown marine macroalgae *Padina tetrastromatica*. *Energy Convers. Manag.* **2017**, *135*, 351–361. [CrossRef]

32. Kalavathy, G.; Baskar, G. Synergism of clay with zinc oxide as nanocatalyst for production of biodiesel from marine *Ulva lactuca*. *Bioresour. Technol.* **2019**, *281*, 234–238. [CrossRef]

33. Khan, A.; Fatima, N. Biodiesel synthesis via metal oxides and metal chlorides catalysis from marine alga *Melanothamnus afaqhusainii*. *Chin. J. Chem. Eng.* **2016**, *24*, 388–393. [CrossRef]

34. Khan, A.M.; Fatima, N.; Hussain, M.S.; Yasmeen, K. Biodiesel production from green seaweed Ulva fasciata catalyzed by novel waste catalysts from Pakistan Steel Industry. *Chin. J. Chem. Eng.* **2016**, *24*, 1080–1086. [CrossRef]

35. Khan, A.M.; Obaid, M.; Shah, M.R. Nanocatalyzed biodiesel synthesis from the oily contents of Marine brown alga Dictyota dichotoma. *Int. J. Green Energy* **2017**, *14*, 925–933. [CrossRef]

36. Saengsawang, B.; Bhuyar, P.; Manmai, N.; Ponnusamy, V.K.; Ramaraj, R.; Unpaprom, Y. The optimization of oil extraction from macroalgae, Rhizoclonium sp. by chemical methods for efficient conversion into biodiesel. *Fuel* **2020**, *274*, 117841. [CrossRef]

37. Sivaprakash, G.; Mohanrasu, K.; Ananthi, V.; Jothibasu, M.; Nguyen, D.D.; Ravindran, B.; Chang, S.W.; Nguyen-Tri, P.; Tran, N.H.; Sudhakar, M.; et al. Biodiesel production from Ulva linza, Ulva tubulosa, Ulva fasciata, Ulva rigida, Ulva reticulate by using Mn2ZnO4 heterogenous nanocatalysts. *Fuel* **2019**, *255*, 115744. [CrossRef]

38. Suganya, T.; Gandhi, N.N.; Renganathan, S. Production of algal biodiesel from marine macroalgae Enteromorpha compressa by two step process: Optimization and kinetic study. *Bioresour. Technol.* **2013**, *128*, 392–400. [CrossRef]

39. Xu, X.; Kim, J.Y.; Oh, Y.R.; Park, J.M. Production of biodiesel from carbon sources of macroalgae, Laminaria japonica. *Bioresour. Technol.* **2014**, *169*, 455–461. [CrossRef]

40. Kostas, E.T.; Adams, J.M.M.; Ruiz, H.A.; Durán-Jiménez, G.; Lye, G.J. Macroalgal biorefinery concepts for the circular bioeconomy: A review on biotechnological developments and future perspectives. *Renew. Sustain. Energy Rev.* **2021**, *151*, 111553. [CrossRef]

41. Cubides-Román, D.C.; Perez, V.H.; Castro, H.F.d.; Orrego, C.E.; Giraldo, O.; Silveira, E.G.; David, G.F. Ethyl esters (biodiesel) production by *Pseudomonas fluorescens* lipase immobilized on chitosan with magnetic properties in a bioreactor assisted by electromagnetic field. *Fuel* **2017**, *196*, 481–487. [CrossRef]

42. de Andrade, C.M.; Cogo, A.J.D.; Perez, V.H.; Santos, N.F.d.; Okorokova-Façanha, A.L.; Justo, O.R.; Façanha, A.R. Increases of bioethanol productivity by *S. cerevisiae* in unconventional bioreactor under ELF-magnetic field: New advances in the biophysical mechanism elucidation on yeasts. *Renew. Energy* **2021**, *169*, 836–842. [CrossRef]

43. Dussan, K.; Justo, O.; Perez, V.; David, G.; Junior, E.S.; da Silva, S. Bioethanol Production From Sugarcane Bagasse Hemicellulose Hydrolysate by Immobilized *S. shehatae* in a Fluidized Bed Fermenter Under Magnetic Field. *Bio. Energy Res.* **2019**, *12*, 338–346. [CrossRef]

44. Junior, E.G.S.; Justo, O.R.; Perez, V.H.; Melo, F.d.; Reyero, I.; Serrano-Lotina, A.; Mompean, F.J. Biodiesel synthesis using a novel monolithic catalyst with magnetic properties (K_2CO_3/γ-Al_2O_3/Sepiolite/γ-Fe_2O_3) by ethanolic route. *Fuel* **2020**, *271*, 117650. [CrossRef]

45. Junior, E.G.S.; Justo, O.R.; Perez, V.H.; Reyero, I.; Serrano-Lotina, A.; Ramirez, L.C.; dos Santos Dias, D.F. Extruded Catalysts with Magnetic Properties for Biodiesel Production. *Adv. Mater. Sci. Eng.* **2018**, *2018*, 3980967.

46. Guiochon, G.; Guillemin, C.L. Chapter 13 Quantitative Analysis By Gas Chromatography Basic Problems, Fundamental Relatio ships, Measurement of the Sample Size. In *Journal of Chromatography Library*; Guiochon, G., Guillemin, C.L., Eds.; Elsevier: Amsterdam, The Netherlands, 2018; pp. 563–586.

47. Barrett, E.P.; Joyner, L.G.; Halenda, P.P. The Determination of Pore Volume and Area Distributions in Porous Substances. I. Computations from Nitrogen Isotherms. *J. Am. Chem. Soc.* **1951**, *73*, 373–380. [CrossRef]

48. Brunauer, S.; Emmett, P.H.; Teller, E. Adsorption of Gases in Multimolecular Layers. *J. Am. Chem. Soc.* **1938**, *60*, 309–319. [CrossRef]

49. Veeranan, T.; Kasirajaan, R.; Gurunathan, B.; Sahadevan, R. A novel approach for extraction of algal oil from marine macroalgae Ulva fasciata. *Renew. Energy* **2018**, *127*, 64–73. [CrossRef]

50. Habibi, M.H.; Parhizkar, J. Cobalt ferrite nano-composite coated on glass by Doctor Blade method for photo-catalytic degradation of an azo textile dye Reactive Red 4: XRD, FESEM and DRS investigations, Spectrochimica acta. Part A. *Mol. Biomol. Spectrosc.* **2015**, *150*, 879–885. [CrossRef] [PubMed]

51. Kooti, M.; Sedeh, A.N.; Gheisari, K.; Figuerola, A. Synthesis, characterization, and performance of nanocomposites containing reduced graphene oxide, polyaniline, and cobalt ferrite. *Phys. B Condens. Matter* **2021**, *612*, 412974. [CrossRef]

52. Helmi, F.; Helmi, M.; Hemmati, A. Phosphomolybdic acid/chitosan as acid solid catalyst using for biodiesel production from pomegranate seed oil via microwave heating system: RSM optimization and kinetic study. *Renew. Energy* **2022**, *189*, 881–898. [CrossRef]

53. Salim, S.M.; Izriq, R.; Almaky, M.M.; Al-Abbassi, A.A. Synthesis and characterization of ZnO nanoparticles for the production of biodiesel by transesterification: Kinetic and thermodynamic studies. *Fuel* **2022**, *321*, 124135. [CrossRef]

54. Zhu, Z.; Liu, Y.; Cong, W.; Zhao, X.; Janaun, J.; Wei, T.; Fang, Z. Soybean biodiesel production using synergistic CaO/Ag nano catalyst: Process optimization, kinetic study, and economic evaluation. *Ind. Crop. Prod.* **2021**, *166*, 113479. [CrossRef]

55. Kamran, E.; Mashhadi, H.; Mohammadi, A.; Ghobadian, B. Biodiesel production from Elaeagnus angustifolia.L seed as a novel waste feedstock using potassium hydroxide catalyst. *Biocatal. Agric. Biotechnol.* **2020**, *25*, 101578. [CrossRef]

56. Liu, J.-Z.; Cui, Q.; Kang, Y.-F.; Meng, Y.; Gao, M.-Z.; Efferth, T.; Fu, Y.-J. Euonymus maackii Rupr. Seed oil as a new potential non-edible feedstock for biodiesel. *Renew. Energy* **2019**, *133*, 261–267. [CrossRef]

57. Xu, W.; Ge, X.-d.; Yan, X.-h.; Shao, R. Optimization of methyl ricinoleate synthesis with ionic liquids as catalysts using the response surface methodology. *Chem. Eng. J.* **2015**, *275*, 63–70. [CrossRef]

58. Zhao, R.; Yang, X.; Li, M.; Peng, X.; Wei, M.; Zhang, X.; Yang, L.; Li, J. Biodiesel preparation from *Thlaspi arvense* L. seed oil utilizing a novel ionic liquid core-shell magnetic catalyst. *Ind. Crops Prod.* **2021**, *162*, 113316. [CrossRef]

59. Chen, G.; Liu, J.; Yao, J.; Qi, Y.; Yan, B. Biodiesel production from waste cooking oil in a magnetically fluidized bed reactor using whole-cell biocatalysts. *Energy Convers. Manag.* **2017**, *138*, 556–564. [CrossRef]

60. Jnaneshwara, D.; Avadhani, D.; Prasad, B.D.; Nagabhushana, B.; Nagabhushana, H.; Sharma, S.; Shivakumara, C.; Rao, J.; Gopal, N.; Ke, S.-C.; et al. Electron paramagnetic resonance, magnetic and electrical properties of CoFe2O4 nanoparticles. *J. Magn. Magn. Mater.* **2013**, *339*, 40–45. [CrossRef]

61. Krishnan, S.G.; Pua, F.-L.; Zhang, F. A review of magnetic solid catalyst development for sustainable biodiesel production. *Biomass Bioenergy* **2021**, *149*, 106099. [CrossRef]

62. Bauer, L.M.; Costa, J.A.V.; da Rosa, A.P.C.; Santos, L.O. Growth stimulation and synthesis of lipids, pigments and antioxidants with magnetic fields in Chlorella kessleri cultivations. *Bioresour. Technol.* **2017**, *244*, 1425–1432. [CrossRef]

63. Chu, F.-J.; Wan, T.-J.; Pai, T.-Y.; Lin, H.-W.; Liu, S.-H.; Huang, C.-F. Use of magnetic fields and nitrate concentration to optimize the growth and lipid yield of Nannochloropsis oculata. *J. Environ. Manag.* **2020**, *253*, 109680. [CrossRef]

64. Costa, S.S.; Peres, B.P.; Machado, B.R.; Costa, J.A.V.; Santos, L.O. Increased lipid synthesis in the culture of *Chlorella homosphaera* with magnetic fields application. *Bioresour. Technol.* **2020**, *315*, 123880. [CrossRef] [PubMed]

65. Feng, X.; Chen, Y.; Lv, J.; Han, S.; Tu, R.; Zhou, X.; Jin, W.; Ren, N. Enhanced Lipid Production by *Chlorella pyrenoidosa* through Magnetic Field Pretreatment of Wastewater and Treatment of Microalgae-wastewater Culture Solution: Magnetic Field Treatment Modes and Conditions. *Bioresour. Technol.* **2020**, *306*, 123102. [CrossRef] [PubMed]

66. Small, D.P.; Hüner, N.P.A.; Wan, W. Effect of static magnetic fields on the growth, photosynthesis and ultrastructure of *Chlorella kessleri* microalgae. *Bioelectromagnetics* **2012**, *33*, 298–308. [CrossRef]

67. Lau, C.H.; Gan, S.; Lau, H.L.N.; Lee, L.Y.; Thangalazhy-Gopakumar, S.; Ng, H.K. Insights into the effectiveness of synthetic and natural additives in improving biodiesel oxidation stability. *Sustain. Energy Technol. Assess.* **2022**, *52*, 102296. [CrossRef]

68. Rajamohan, S.; Gopal, A.H.; Muralidharan, K.R.; Huang, Z.; Paramasivam, B.; Ayyasamy, T.; Nguyen, X.P.; Le, A.T.; Hoang, A.T. Evaluation of oxidation stability and engine behaviors operated by Prosopis juliflora biodiesel/diesel fuel blends with presence of synthetic antioxidant. *Sustain. Energy Technol. Assess.* **2022**, *52*, 102086. [CrossRef]

69. Silva, W.C.; Castro, M.P.P.; Perez, V.H.; Machado, F.A.; Mota, L.; Sthel, M.S. Thermal degradation of ethanolic biodiesel: Physicochemical and thermal properties evaluation. *Energy* **2016**, *114*, 1093–1099. [CrossRef]

70. da Silva, J.C.M.; Nicolau, C.L.; Cabral, M.R.P.; Costa, E.R.; Stropa, J.M.; Silva, C.A.A.; Scharf, D.R.; Simionatto, E.L.; Fiorucci, A.R.; de Oliveira, L.C.S.; et al. Thermal and oxidative stabilities of binary blends of esters from soybean oil and non-edible oils (*Aleurites moluccanus*, *Terminalia catappa*, and *Scheelea phalerata*). *Fuel* **2020**, *262*, 116644. [CrossRef]

71. Nicolau, C.L.; Klein, A.F.V.; Silva, C.A.A.; Fiorucci, A.R.; Stropa, J.M.; Santos, E.; Simionatto, E. Thermal Properties of the Blends of Methyl and Ethyl Esters Prepared from Babassu and Soybean Oils. *J. Braz. Chem. Soc.* **2018**, *29*, 1672–1679. [CrossRef]

72. Zhou, G.-x.; Chen, G.-y.; Yan, B.-b. Biodiesel production in a magnetically-stabilized, fluidized bed reactor with an immobilized lipase in magnetic chitosan microspheres. *Biotechnol. Lett.* **2014**, *36*, 63–68. [CrossRef]